

Direct flue gas CO₂ mineralization using activated serpentine: Exploring the reaction kinetics by experiments and population balance modelling

Conference Paper**Author(s):**

Werner, Mischa; Verduyn, Marcel; van Mossel, Gert; Mazzotti, Marco

Publication date:

2011

Permanent link:

<https://doi.org/10.3929/ethz-b-000163056>

Rights / license:

[Creative Commons Attribution-NonCommercial-NoDerivs 3.0 Unported](#)

Originally published in:

Energy Procedia 4, <https://doi.org/10.1016/j.egypro.2011.02.086>



GHGT-10

Direct flue gas CO₂ mineralization using activated serpentine: Exploring the reaction kinetics by experiments and population balance modelling

Mischa Werner^a, Marcel Verduyn^b, Gert van Mossel^b and Marco Mazzotti^{a,*}^a*Institute of Process Engineering, ETH Swiss Federal Institute of Technology, Sonneggstrasse 3, CH-8092 Zurich, Switzerland*^b*Shell Global Solutions International B.V., PO Box 38000, NL-1031 HW, Amsterdam, the Netherlands*

Abstract

Avoiding CO₂ emissions to the atmosphere by its safe and permanent storage is required for all options within the CCS framework. Only mineral carbonation allows for a sequestration process, where the carbon is rapidly converted to its chemically most stable form, a carbonate. So far, most researchers looking into mineral carbonation focused on routes that involve an aqueous medium, where carbonation takes place under an atmosphere of pure CO₂, either in a single or multi-step process. We have started to investigate a novel approach to aqueous mineral carbonation where the costly capture step is avoided by the direct mineralization of flue gas CO₂ at the point source. For the present study, we have built a set-up to perform mineralization experiments under a variety of conditions in both batch or flow-through mode. The residence times of the reactor solution and gas phase involved can be freely adjusted: the design allows for flowing both the feed solution and the flue gas continuously through an autoclave that contains a sample of activated serpentine. The use of online ion chromatography and in-situ Raman spectroscopy allows monitoring magnesium concentration as well as the solids and dissolved phases throughout an experimental run. A population balance equation model has been developed and its solution was coupled with the continuous flow-through reactor model. The experimental data serves as input to the model in order to regress reaction rates under a variety of operating conditions. A precise knowledge of the dissolution and precipitation kinetics is required for the optimal design and scale-up of the mineralization process. Moreover, the ultimate particle size distribution is of key importance for mineralization product processing and product applications.

© 2011 Published by Elsevier Ltd. Open access under [CC BY-NC-ND license](https://creativecommons.org/licenses/by-nc-nd/4.0/).

Keywords: Mineral carbonation; Serpentine; Flue gas; Kinetics; Population balance

1. Introduction to the flue gas mineralization concept

To date, a variety of mineralization routes have been suggested, some successfully tested at laboratory scale, some even patented. Each route involves the pre-treatment of a magnesium or calcium oxide bearing material, its

* Corresponding author. Tel.: +41-44-632-2456; fax: +41-44-632-1141.

E-mail address: marco.mazzotti@ipe.mavt.ethz.ch

carbonation (Mg/Ca-leaching followed by carbonate precipitation) and further processing steps downstream. The products can be used given a market exists or deposited without the need of a measurement, monitoring, and verification (MMV) program [1]. Owing to the high prize per ton of CO₂ sequestered, mineralization has received little attention within the CCS community. Obviously, current cost estimations fail to monetize and internalize the benefit of having CO₂ stored in solid, environmentally benign form. Removing CO₂ from an industrial off-gas at the point source accounts for 80-90% of the overall costs of the CCS value chain that conventionally includes CO₂ capture, compression, transport, geological storage, and MMV on site [1]. While costs for providing pure CO₂ to a mineral carbonation plant or to a geological storage site are the same, the energy input needed for fast mineralization rates in the reactor will most likely lead to higher costs than those associated with a successful geological storage operation. The only way to circumvent this cost imbalance is to skip the conventional capture and transport step and to extract CO₂ directly out of the flue gas by a mineralization process adapted to low CO₂ partial pressures. As summarized in Table 1, this concept has so far been applied to alkaline industrial residues as raw material, but barely to the more abundant but less reactive natural minerals.

Table 1: Recent literature on flue gas CO₂ mineralization.

	Direct carbonation (single-step)		Staged carbonation (multi-step)	
	Industrial residues	Natural minerals	Industrial residues	Natural minerals
Dry carbonation	[2-3]	No literature	[4]	No literature
Aqueous carbonation	[5-6]	No literature	[6-8]	[9-11]

We have started to bring our work on aqueous mineral carbonation [12-15] in line with the work presented in Verduyn et al. (2006) [16], namely to investigate the use of flue gas with natural minerals experimentally and based on model simulations. Magnesium silicates, such as serpentines, are worldwide the most abundant source of metal oxides that can form mineral carbonates [17]. Any process design for conventional aqueous mineral carbonation needs to resolve two trade-offs. Firstly, more CO₂ could dissolve into the aqueous phase if temperature was low, but both the dissolution of the raw material and the precipitation of carbonates are favoured at elevated temperature levels. Secondly, an acidic environment (low pH) would indeed accelerate the Mg-/Ca-leaching through proton-exchange reaction, but high supersaturation levels with respect to the Mg-/Ca-carbonates is reached fastest at alkaline conditions (high pH), where the carbonic acid prevails in fully deprotonated form. One way to address these trade-offs is to increase the operating CO₂ pressures. This promotes the solubility of CO₂ into solution, which leads to an increased activity of all species within the carbonic acid equilibrium (both protonated and deprotonated). High-pressure levels, however, are not feasible for the flue gas concept, since co-pressurization of virtually 90% non-CO₂ off-gas would be detrimental for process efficiency. Our approach is to contact cooled flue gas with the raw mineral during wet-grinding and leaching, followed by precipitation at increased temperature, where carbonate solubility is low [16]. In Figure 1 this concept is visualized schematically along with the conventional approach mentioned above.

To ensure that all feed gas is converted rapidly into solid product, an aqueous carbonation plant running on pure CO₂ would require a gas tight reactor design up to high-pressure levels. Conversely, a plant after the novel approach would include contactors that are flown-through by flue gas at fairly low temperature and pressure levels. Under moderate conditions magnesium silicate dissolution is slow (e.g. in [18]). However, since it circumvents the energy effort for capture, the flue gas mineralization concept leaves room for energy intensive mechanical (attrition grinding) and thermal activation. The latter has been shown to promote serpentine carbonation by factor 5 [19]. An initial techno-economic assessment has shown that the transition from pure CO₂ to flue gas mineralization using serpentines looks technically feasible and a preliminary step cost analysis foreshadows the compressibility of the abatement costs.

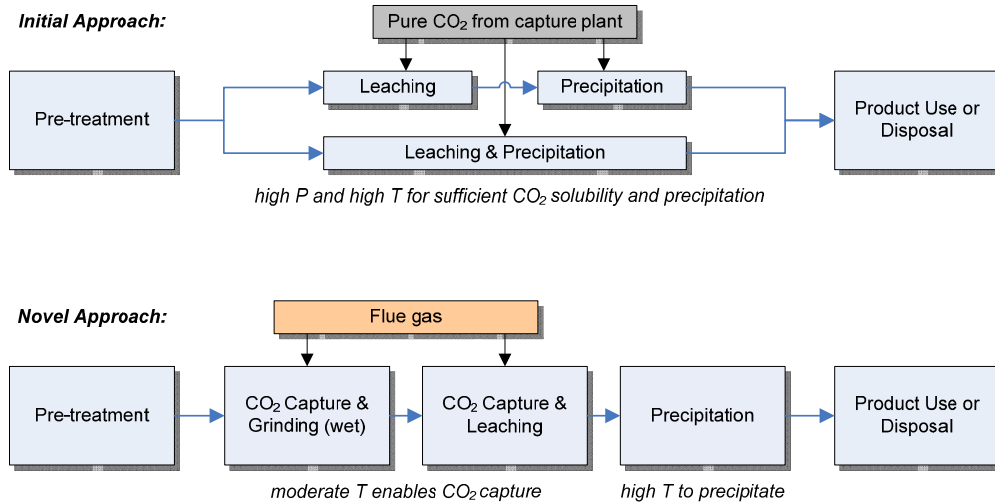


Figure 1: Concept of direct flue gas CO₂ mineralization in comparison with initial approach (after [16]).

2. Material and experimental set-up

The material under investigation is a serpentine rock provided by Shell Global Solutions International, Amsterdam, the Netherlands. The serpentine was received already ground and thermally activated according to the providers standard operating procedure. The magnesium-iron ratio (Mg:Fe) of the original material is 4.22, as determined by XRF analysis. Further material characterization was performed at ETH, including density, particle size distribution (PSD), and BET surface measurements. The density of the activated material was measured at $2629 \pm 2 \text{ kg m}^{-3}$ by helium pycnometry (Micrometrics, AccuPyc 1330). The serpentine powder was wet sieved into three fractions using a $20\mu\text{m}$ and $63\mu\text{m}$ lab sieve and then dried in an oven overnight at 60°C . Particle size distribution of the 20-63 μm fraction was determined in a 0.15 M NaCl solution using a Coulter counter (Beckman, Coulter Multisizer 3). Distribution data were averaged over 9 measurements. Adding 0.005 M sodiumdodecylsulfate (SDS) as dispersant caused no shift of the PSD to smaller particle sizes. The BET specific surface analysis is currently delayed owing to device malfunctioning.

The experimental set-up as described in Hänchen et al. (2006) [12] was disassembled and redesigned to allow for dissolution and carbonation experiments in both batch and flow-through mode, while residence times of aqueous and gaseous phase can be varied independently. The flow rate of flue gas can be set depending on the desired residence time, and on the investigated operating temperatures and pressures. They cover the range from 30 to 180°C and from ambient pressure to 150bar, respectively. The heart of the set-up is a 300ml titanium autoclave placed in an oil bath with external temperature control. This oil bath is mounted on a high-capacity, low-readability balance (Mettler, XS64001LX). The lid hosts in- and outlet for liquid and gaseous flows, pressure and temperature sensors, a rupture disk, and a probe for in-situ monitoring via Raman spectroscopy (Kaiser, RXN1-789). Pressure is controlled by means of a backpressure regulator (BPR), while gas mass flow is set upstream via a mass flow controller. The flue gas inlet to the autoclave is a gas dispersion stirrer, which is connected to two bottles: the nitrogen bottle (grad 5, 99.999% pure) is used for the heat up period prior to an experimental run, the second bottle contains a mixture of 10%_{mol} CO₂ (grade 4.5, 99.995% pure) in N₂, resembling the composition of flue gas from a coal and gas fired power plant (in average). This mixture is lacking the moisture of a real flue gas, thus stripping water when flown through the reactor. The pipes downstream are therefore heated to prevent condensation. The excess water vapor is removed to a big extent in a condenser after the BPR, prior to online gas analysis via mass spectrometry further downstream (Pfeiffer Vacuum, GSD 301 C1). As carbonation of the serpentine in the reactor proceeds, magnesium ions (Mg²⁺) are leached out from the silicate into solution and consumed thereafter by

carbonate precipitation. To measure the concentration developing of Mg^{2+} throughout an experimental run, a small liquid stream is withdrawn by means of an HPLC pump and piped to online analysis via ion chromatography (Dionex, ICS-2000, CS12A column). Upstream, another HPLC pump delivers the necessary make-up of feed solution, in order to maintain a constant liquid level in the reactor. Constant flow is ensured via mass flow regulation at the inlet and the adjustment of the outlet pump rate according to the signal of the balance that detects weight changes in the reactor.

Earlier, we have measured and reported kinetic data about the dissolution of olivine [12-13, 15]. At that time, experiments were run under elevated pressure levels using pure CO_2 . Thus, only make up gas was needed to maintain pressure. The make-up was fed from a buffer tank via front pressure regulator into the reactor. Also today, in addition to the gas flow through design, it is possible to run high pressure experiments using pure CO_2 . This extra was aimed at running experiments that can confirm the current plant's performance by comparing actual runs with data retrieved using the former set-up. Upon completion of the assemblage and testing, a preliminary series of dissolution experiments was performed, the feed material being olivine instead of serpentine. Sample size and operating conditions were chosen to match the experimental conditions reported in [15].

3. Population balance equation modelling

We have developed models, based on population balance equations (PBE), where the obtained data will serve for parameter estimation and process simulation. A PBE describes the number of crystals in a given size range ΔL over the time interval Δt . Crystal size is parameterized using a characteristic particle length L , which has to be related to a physical property of the particles. It is convenient to use Feret diameters, i.e. the distance of two parallel tangent planes on a particle. The number of crystals can then be expressed by the PSD:

$$n(t, L) = \frac{dN}{dL}. \quad (1)$$

The PSD represents the unscaled number distribution density of the particle population. With $N(L)$ being the cumulative particle size distribution, $n(t, L)dL$ returns the concentration of particles at given time t in the size range L to $L+dL$. For the sake of simplicity, spatial complexity of the true particle shape was reduced to a 1-D model, characterizing size and shape simultaneously using only one parameter, i.e. L . Therefore, the dimensionless shape factor, k_v , was defined to relate the cube of side length L to its volume v [20]:

$$v = k_v L^3. \quad (2)$$

Generally, k_v has to be estimated from image analysis for each kind of particles. In the context of a 1-D model, they are assumed to be time-invariant and size-independent, which is only true under the constraint of isotropic particle dissolution and growth. The total volume $V(t)$ for a given particle population can be derived by introducing the concept of the moments of a distribution. The j^{th} moment of the PSD of the i^{th} material, $n_i(t, L_i)$, is defined as:

$$\mu_i^j(t) = \int_0^\infty L^j n_i(t, L_i) dL. \quad (3)$$

Only the first four moments are related to a physical meaning, namely the zeroth (μ_i^0) to the total number of particles, the first (μ_i^1) to the cumulative length of all particles, the second (μ_i^2) to the total surface area and the third (μ_i^3) to the total volume of the population. Using these properties, one can write:

$$V_i(t) = k_{v,i} \mu_i^3(t). \quad (4)$$

The definition of the dissolution rate R and growth rate G is given by the infinitesimal change of L over time ($m s^{-1}$), which is negative for R and positive for G , respectively:

$$R = G = \frac{dL}{dt}. \quad (5)$$

Recalling the definition of $N(L)$ from Eq. 1, the nucleation rate J is defined as the change of the number of particles over time at $L = 0$:

$$J = \left. \frac{dN}{dt} \right|_{L=0}. \quad (6)$$

Thus, the final population balances write [20]:

$$\frac{\partial n_d}{\partial t} - R \frac{\partial n_d}{\partial L_d} = 0, \quad (7)$$

$$\frac{\partial n_p}{\partial t} - G \frac{\partial n_p}{\partial L_p} = 0, \quad (8)$$

with subscript d and p indicating the dissolution and precipitation part, respectively. Initial and boundary conditions for the two homogeneous partial differential equations (first-order wave equations) are:

$$n_d(0, L_d) = n_d^0(L_d), \quad (9)$$

$$n_d(t, 0) = n_d^0(\lambda), \quad (10)$$

$$n_p(0, L_p) = 0, \quad (11)$$

$$n_p(t, 0) = \frac{J}{G}, \quad (12)$$

with $n_d^0(\lambda)$ representing the number of particles at time t that are dissolving completely. The corresponding characteristic length λ follows from the integral of the dissolution rate R :

$$\lambda = \left| \int_0^{\lambda} R dt \right|. \quad (13)$$

The solution to the PBEs was coupled with a reactor model. The mass balance for the concentration of the total magnesium in solution, $c_{Mg(aq)}$ (M), was formulated to be applicable for a continuous flow stirred tank reactor (CFSTR). It is given by:

$$V \frac{dc_{Mg(aq)}}{dt} = v \frac{dm_d}{dt} - \frac{dm_p}{dt} - Q c_{Mg(aq)}, \quad (14)$$

where V (ml) is the liquid volume in the reactor, v is the number of moles of magnesium in one mole of serpentine, m_d and m_p (mol) are the masses of solute and precipitate, and Q (ml min⁻¹) is the flow rate through the reactor. The partial differential equations (PDE), Eqs. 7-8, have been solved using the method of moments. The two PBEs were transformed into a set of coupled ordinary differential equations (ODEs), consisting of the time derivatives of the first four moments of the PSD. Starting with the zeroth moment, this writes for the serpentine dissolution:

$$\frac{d\mu_d^0}{dt} = R n_d^0(\lambda), \quad (15)$$

$$\frac{d\mu_d^1}{dt} = R \mu_d^0, \quad (16)$$

$$\frac{d\mu_d^2}{dt} = 2R \mu_d^1, \quad (17)$$

$$\frac{d\mu_d^3}{dt} = 3R \mu_d^2. \quad (18)$$

For the Mg-carbonate precipitation, the derivative of the 0th moment writes:

$$\frac{d\mu_p^0}{dt} = J, \quad (19)$$

while the consecutive derivatives for the first to the third moment are of the same form as given in Eq. 16-18, except for the change in subscript (d becomes p) and for the dissolution rate R becoming the growth rate G . Using the time derivatives of the third moment in integral form, i.e. the total volume of the particles, the mass balance in Eq. 14 can be written as follows:

$$\frac{dc_{Mg(aq)}}{dt} = v 3k_{v,d} \rho_d R \int_0^{\infty} n_d L_d^2 dL - 3k_{v,p} \rho_p G \int_0^{\infty} n_p L_p^2 dL - \frac{Q}{V} c_{Mg(aq)}, \quad (20)$$

where ρ_d and ρ_p (mol m⁻³) are the molar densities of serpentine and Mg-carbonate, respectively. The ODEs in Eqs. 15-20 were solved using the Matlab solver ode15s.

4. Results set-up verification

The new set-up was successfully commissioned and tested this summer. Previously published measurements of olivine dissolution kinetics were reproduced successfully during the test phase. Figure 2 shows the comparison of an old experiment, Exp. no° R92 [15], with a current run, Exp. no° M3, where the experimental conditions were kept exactly alike; namely the temperature at 120°C, the total pressure at 100bar, and the initial sample mass being as low as 11.35mg of ground olivine from the 90-180µm fraction, in order to stay at far from equilibrium dissolution conditions.

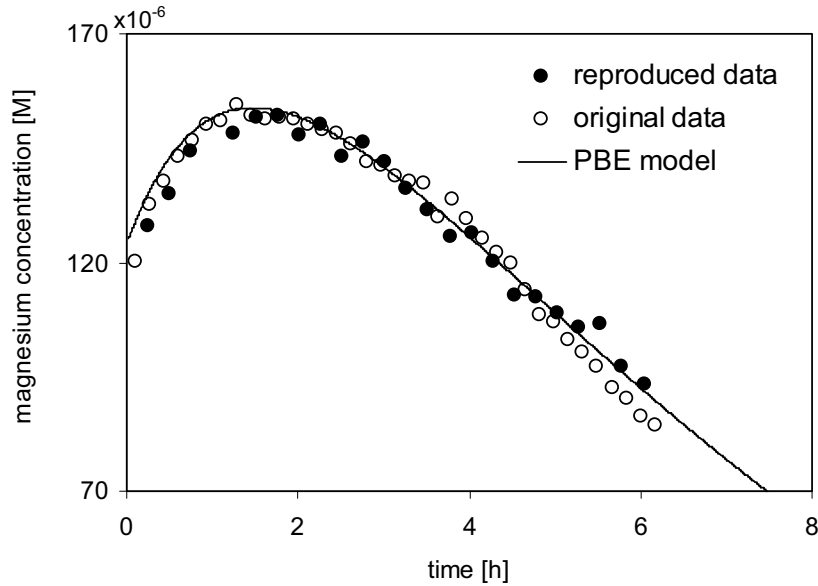


Figure 2: Comparison of the measured magnesium concentration during an old experiment (empty disks = Exp. No° R92 in [15]) with the corresponding reproducibility test run (filled disks, Exp. No° M3), along with the PBE model simulation (solid line). Experimental conditions: $m_0=11.35\text{mg}$, $T=120^\circ\text{C}$, $P_{\text{tot}}=100\text{bar}$.

Acknowledgements:

This work is funded by Shell Global Solutions International B.V., PO Box 38000, NL-1031 HW Amsterdam, the Netherlands.

References

- [1] IPCC. Special report on carbon dioxide capture and storage. Cambridge and New York: Cambridge University Press; 2005.
- [2] Prigiobbe V, Poletini A, Baciocchi R. Gas-solid carbonation kinetics of Air Pollution Control residues for CO₂ storage. *Chem Eng J* 2009;148(2-3):270-8.
- [3] Reddy KJ, Argyle MD, Viswatej A. Capture and mineralization of flue gas carbon dioxide (CO₂). In: Baciocchi R, Costa G, Poletini A, Pomi R, editors. 2nd international Conference on Accelerated Carbonation for Environmental and Materials Engineering, Rome; 2008, p. 221-5.
- [4] Lin PC, Huang CW, Hsiao CT, Teng H. Magnesium hydroxide extracted from a magnesium-rich mineral for CO₂ sequestration in a gas-solid system. *Environ Sci Technol* 2008;42(8):2748-52.
- [5] Sun J, Fernandez-Bertos M, Simons SJR. Kinetic study of accelerated carbonation of municipal solid waste incinerator air pollution control residues for sequestration of flue gas CO₂. *Energy Environ Sci* 2008;1:370-7.
- [6] Uibu M, Velts O, Kuusik R. Developments in CO₂ mineral carbonation of oil shale ash. *J Hazard Mater* 2010;174(1-3):209-14.
- [7] Geerlings JJC, van Mossel GAF, in't Veen BCM. Process for producing CaCO₃ or MgCO₃. WO2006008242(A1), CN1989073 (A), US2007202032 (A1); Shell Oil Company; 2006.
- [8] Kodama S, Nishimoto T, Yamamoto N, Yogo K, Yamada K. Development of a new pH-swing CO₂ mineralization process with a recyclable reaction solution. *Energy* 2008;33(5):776-84.
- [9] Li WZ, Li W, Li B, Bai Z. Electrolysis and heat pretreatment methods to promote CO₂ sequestration by mineral carbonation. *Chem Eng Res Des* 2009;87(2):210-5.
- [10] Hunwick RJ. System, apparatus and method for carbon dioxide sequestration. WO2008101293 (A1), US2010021362 (A1), KR20090125109 (A), EP2134449 (A1), CA2678800 (A1), AU2009250983 (A1); 2008.
- [11] Geerlings JJC, Wesker E. A process for sequestration of carbon dioxide by mineral carbonation. WO2008142017 (A2) (A3), EP2158158 (A2), CA2687618 (A1), AU2008253068 (A1), US20070261947 (A1), CN101679059 (A); Shell Internationale Research Maatschappij B.V.; 2008.
- [12] Hänchen M, Prigiobbe V, Storti G, Seward TM, Mazzotti M. Dissolution kinetics of forsteritic olivine at 90-150 °C including effects of the presence of CO₂. *Geochim Cosmochim Acta* 2006;70(17): 4403-16.
- [13] Hänchen M, Krevor S, Lackner KS, Mazzotti M. Validation of a population balance model for olivine dissolution. *Chem Eng Sci* 2007;62(22):6412-22.
- [14] Hänchen M, Prigiobbe V, Baciocchi R, Mazzotti M. Precipitation in the Mg-carbonate system--effects of temperature and CO₂ pressure. *Chem Eng Sci* 2008;63(4):1012-28.
- [15] Prigiobbe V, Costa G, Baciocchi R, Hänchen M, Mazzotti M. The effect of CO₂ and salinity on olivine dissolution kinetics at 120°C. *Chem Eng Sci* 2009;64(15):3510-15.
- [16] Verduyn MA, Boerringer H, Oudwater R, van Mossel GAF. A Novel Process Concept for CO₂ Mineralization; Technical Opportunities and Challenges. In: 5th Trondheim Conference on CO₂ Capture, Transport and Storage, Trondheim; 2009.
- [17] Lackner KS. CLIMATE CHANGE: A guide to CO₂ sequestration. *Science* 2003;300(5626):1677-8.
- [18] Pokrovsky OS, Schott J. Kinetics and mechanism of forsterite dissolution at 25°C and pH from 1 to 12. *Geochim Cosmochim Acta* 2000;64(19):3313-25.
- [19] O'Connor WK, Dahlin DC, Rush GE, Gerdemann SJ, Penner LR, Nilsen DN. Aqueous mineral carbonation: Mineral availability, pretreatment, reaction parameters, and process studies. Albany Research Center, DOE/ARC-TR-04-002, final report; 2005.
- [20] Randolph A, Larson MA. Theory of particulate processes. 2nd ed. San Diego: Academic Press; 1988.